Open Access Journal

Journal of Power Technologies 95 (4) (2015) 309–316

journal homepage:papers.itc.pw.edu.pl

Method of determination of thermo-flow parameters for steam boiler☆

Jan Taler[a,*], Bohdan Węglowski[a], Dawid Taler[b], Marcin Trojan[a], Tomasz Sobota[a], Piotr Dzierwa[a], Marcin Pilarczyk[a], Paweł Madejski[c], Daniel Nabagło[c]

[a]*Cracow University of Technology, Faculty of Mechanical Engineering, Institute of Thermal Power Engineering, Al. Jana Pawła II 37, 31-864 Cracow, Poland;*
[b]*Cracow University of Technology, Faculty of Environmental Engineering, Institute of Thermal Engineering and Air Protection, Warszawska 24, 31-155 Cracow, Poland;*
[c]*EDF Polska S. A., Research and Development, Ciepłownicza 1, 31-587 Cracow, Poland;*

Abstract

The paper presents a method for determining thermo-flow parameters for steam boilers. This method allows one to perform the calculations of the boiler furnace chamber and heat flow rates absorbed by superheater stages. These parameters are important for monitoring the performance of the power unit. Knowledge of these parameters makes it possible to determine the degree of furnace chamber slagging. The calculation can be performed in online mode and used in the monitoring of the steam boiler. The presented method allows the steam boiler to be run at high efficiency.

Keywords: Combustion chamber; Fouling and slagging; Superheaters; Thermal performance monitoring; Heating surfaces

1. Introduction

The fouling processes caused by slagging and ash deposits are strongly affected by the kind of coal used [1–6]. They become more intense if coal is co-fired with biomass. In the case of the furnace chamber, the fouling processes are different on its individual walls. Depending on the furnace chamber aerodynamics, local slag overhangs may be formed in the burner area or at other locations on the chamber walls. In places where the temperature is high, such as the platen superheater area, superheater surface slagging may also be caused by melted drops of ash forming deposits on the surface of tubes [7]. If biomass is co-fired, due to the low melting point of ash, intense processes of ash deposit formation and slagging may occur on the superheater stages located in zones with a lower flue gas temperature.

Ash fouling processes also affect the lifetime of the boiler superheaters [8–10]. It should be noted that about 40% of boiler failures are caused by damage to boiler superheaters.

For this reason, there is a need to develop an effective and efficient method of determination of thermo-flow parameters for steam boilers. The presented method allows the steam boiler to be run at high efficiency.

2. Calculations of the boiler furnace chamber

The degree of fouling of the boiler furnace chamber walls may be assessed by an online mode determination of the flue gas temperature at the furnace chamber outlet T_{fe}, the heat flux absorbed by the furnace chamber walls $\dot{Q}_r$ and the heat effectiveness ψ of the furnace chamber walls. The heat effectiveness ψ of the furnace chamber is defined as an average ratio of the heat flux absorbed by the waterwall to the heat flux falling on the waterwall of the combustion chamber.

☆Conference paper (Research and Development in Power Engineering, December 2015, Warsaw, Poland)

*Corresponding author
Email address: taler@mech.pk.edu.pl (Jan Taler)

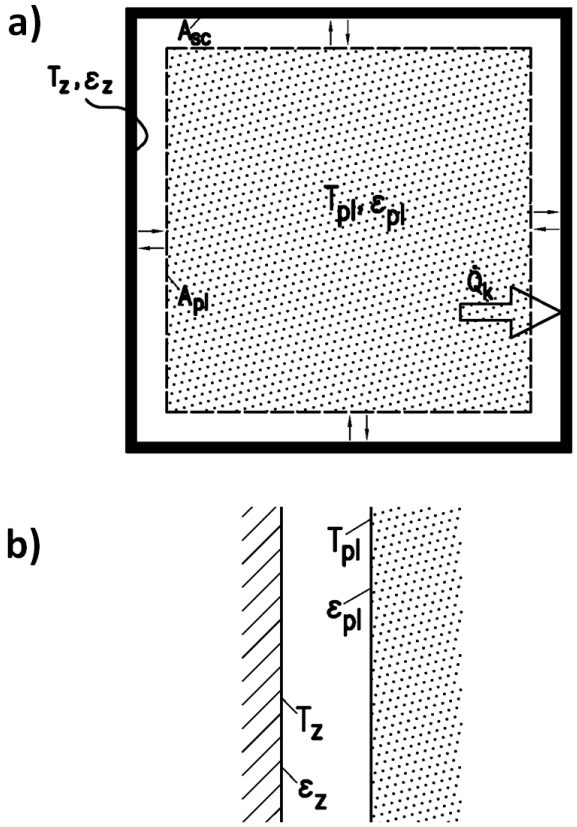

Figure 1: Heat exchange via radiation in the boiler furnace chamber: a) heat exchange between the flame and the furnace chamber walls, b) simplified diagram of heat exchange between the flame and furnace chamber walls

It is assumed that the furnace chamber is filled with a flame with the surface area A_{pl} and emissivity ε_{pl}. The flame temperature is uniform in its entire volume and equal to T_{pl}. The heat flux $\dot{Q}_k$ flows from the flame to the walls with the surface area A_{sc}, temperature T_z and emissivity ε_z (Fig. 1).

The heat flux $\dot{Q}_r$ flowing from flue gases to the furnace chamber walls may be calculated using Formula (1):

$$\dot{Q}_r = \frac{\sigma A_{pl}\left(T_{pl}^4 - T_z^4\right)}{\frac{1}{\varepsilon_{pl}} + \frac{1-\varepsilon_z}{\varepsilon_z}\frac{A_{pl}}{A_{sc}}} \tag{1}$$

where $\sigma = 5.67 \cdot 10^{-8}$ W/(m^2·K^4) is the Stefan-Boltzmann constant.

Considering that in pulverized fuel boilers the flame fills the entire furnace chamber, it may be assumed that the flame surface area A_{pl} is equal to the surface area of the walls A_{sc}. Considering that $A_{pl} = A_{sc}$, Formula (1) is reduced to the following form (Fig. 1b):

$$\dot{Q}_r = \frac{\sigma A_{sc}\left(T_{pl}^4 - T_z^4\right)}{\frac{1}{\varepsilon_{pl}} + \frac{1}{\varepsilon_z} - 1} \tag{2}$$

The effective heat flux transferred from the chamber wall to the furnace is as follows:

$$\dot{q}_{sc,ef} = \varepsilon_z \sigma T_z^4 + (1-\varepsilon_z)\,\dot{q}_{pad} \tag{3}$$

where $\dot{q}_{pad}$ is the density of the heat flux reaching the furnace wall chamber.

The heat flux absorbed by the furnace chamber walls is defined as:

$$\dot{q} = \frac{\dot{Q}_r}{A_{sc}} \tag{4}$$

where $\dot{Q}_r$ is determined by Formula (2).

Introducing the heat efficiency coefficient of the boiler furnace chamber walls ψ:

$$\psi = \frac{\dot{q}}{\dot{q}_{pad}} = \frac{\dot{q}_{pad} - \dot{q}_{sc,ef}}{\dot{q}_{pad}} = 1 - \frac{\dot{q}_{sc,ef}}{\dot{q}_{pad}} \tag{5}$$

the effective heat flux $\dot{q}_{sc,ef}$ is defined as:

$$\dot{q}_{sc,ef} = (1-\psi)\,\dot{q}_{pad} \tag{6}$$

Substitution of (3) in (6) results in:

$$\varepsilon_z \sigma T_z^4 + (1-\varepsilon_z)\,\dot{q}_{pad} = (1-\psi)\,\dot{q}_{pad} \tag{7}$$

which gives the following:

$$\varepsilon_z \sigma T_z^4 = \varepsilon_z \dot{q}_{pad} - \psi \dot{q}_{pad} \tag{8}$$

Introducing $\dot{q} = \psi\,\dot{q}_{pad}$, $\varepsilon_z \sigma T_z^4$ defined by (8) and $\dot{Q}_r$ defined by (2) into Formula (4), after simple transformations, the following equation is obtained:

$$\psi \dot{q}_{pad} = \frac{-\varepsilon_{pl}\left(\varepsilon_z\,\dot{q}_{pad} - \psi\,\dot{q}_{pad}\right) + \varepsilon_z \varepsilon_{pl} \sigma T_{pl}^4}{\varepsilon_{pl} + \varepsilon_z - \varepsilon_z \varepsilon_{pl}} \tag{9}$$

After appropriate transformations, the equation (9) results in the following expression:

$$\varepsilon_{pl} = \frac{1}{1 + \frac{1}{\psi}\left(\frac{\sigma T_{pl}^4}{\dot{q}_{pad}} - 1\right)} \tag{10}$$

The definition of furnace emissivity:

$$\varepsilon_{pal} = \frac{\dot{q}_{pad}}{\sigma T_{pl}^4} \tag{11}$$

gives:

$$\frac{\sigma T_{pl}^4}{\dot{q}_{pad}} = \frac{1}{\varepsilon_{pal}} \tag{12}$$

Substitution of (12) in (10) results in:

$$\varepsilon_{pl} = \frac{1}{1 + \frac{1}{\psi}\left(\frac{1}{\varepsilon_{pal}} - 1\right)} \tag{13}$$

and after more transformations this gives the formula for furnace emissivity:

$$\varepsilon_{pal} = \frac{\varepsilon_{pl}}{\varepsilon_{pl} + \psi\left(1 - \varepsilon_{pl}\right)} \tag{14}$$

The heat flux $\dot{Q}_r$ absorbed by the furnace chamber walls is defined as follows:

$$\dot{Q}_r = A_k\, \dot{q} = A_k\, \dot{q}_{pad}\, \psi = \varepsilon_{pal}\, \psi\, \sigma\, A_k\, T_{pl}^4 \tag{15}$$

In order to calculate the flue gas temperature at the outlet of the furnace chamber T_{fe}, the equation of the energy balance for the boiler furnace chamber is written as:

$$\dot{Q}_r = \dot{Q} - \dot{m}_{sp}\; c_{p,sp}\Big|_0^{T_{fe}-273.15}\left(T_{fe} - 273.15\right) \tag{16}$$

where T_{fe} is the flue gas temperature at the furnace outlet expressed in K.

According to the assumed model of the radiation heat exchange in the furnace chamber, the flue gas temperature in the entire chamber is the same. Therefore, it may be assumed that $T_{fe} = T_{pl}$, where T_{fe} and T_{pl} are expressed in K.

The energy flux $\dot{Q}$ brought to the furnace with fuel and air is:

$$\begin{aligned}\dot{Q} = {} & \dot{m}_{pal}\left(W_d + h_{pal}\right) + \\ & + \dot{m}_{pow}\; c_{p,pow}\Big|_0^{T_{pow}-273.15}\left(T_{pow} - 273.15\right)\end{aligned} \tag{17}$$

where fuel enthalpy h_{pal} is defined as:

$$h_{pal} = c_{p,pal}\Big|_0^{T_{pal}-273.15}\left(T_{pal} - 273.15\right) \tag{18}$$

The heat flux $\dot{Q}$ brought to the furnace may be expressed using the adiabatic combustion temperature (T_{ad}- 273.15).

$$\dot{Q} = \dot{m}_{sp}\; c_{p,sp}\Big|_0^{T_{ad}-273.15}\left(T_{ad} - 273.15\right) \tag{19}$$

where the adiabatic combustion temperature T_{ad} is determined by the following formula:

$$\begin{aligned}T_{ad} = {} & 273.15 + \frac{\dot{m}_{pal}\left(W_d + h_{pal}\right)}{\dot{m}_{sp}\, c_{p,sp}\Big|_0^{T_{ad}-273.15}\left(T_{ad} - 273.15\right)} + \\ & + \frac{\dot{m}_{pow}\, c_{p,pow}\Big|_0^{T_{pow}-273.15}\left(T_{pow} - 273.15\right)}{\dot{m}_{sp}\, c_{p,sp}\Big|_0^{T_{ad}-273.15}\left(T_{ad} - 273.15\right)}\end{aligned} \tag{20}$$

Introducing (15) and (19) into (16), the following is obtained:

$$\begin{aligned}A_k\, \varepsilon_{pal}\, \psi\, \sigma\, T_{fe}^4 = {} & \dot{m}_{sp}\; c_{p,sp}\Big|_0^{T_{ad}-273.15}\left(T_{ad} - 273.15\right) - \\ & - \dot{m}_{sp}\; c_{p,sp}\Big|_0^{T_e-273.15}\left(T_{fe} - 273.15\right)\end{aligned} \tag{21}$$

Introducing the average specific heat of flue gases:

$$\bar{c}_{p,sp} = c_{p,sp}\Big|_{T_{fe}-273.15}^{T_{ad}-273.15} \tag{22}$$

where:

$$\begin{aligned}c_{p,sp}\Big|_{T_{fe}-273.15}^{T_{ad}-273.15} = {} & \frac{c_{p,sp}\Big|_0^{T_{ad}-273.15}\left(T_{ad} - 273.15\right)}{T_{ad} - T_{fe}} - \\ & - \frac{c_{p,sp}\Big|_0^{T_{fe}-273.15}\left(T_{fe} - 273.15\right)}{T_{ad} - T_{fe}}\end{aligned} \tag{23}$$

equation (21) is transformed to the following:

$$A_k\, \varepsilon_{pal}\, \psi\, \sigma\, T_e^4 = \dot{m}_{sp}\, \bar{c}_{p,sp}\left(T_{ad} - T_{fe}\right) \tag{24}$$

After transformations, (24) gives:

$$\frac{T_{fe}}{T_{ad}} = 1 - \frac{\varepsilon_{pal}}{Bo}\left(\frac{T_{fe}}{T_{ad}}\right)^4 \tag{25}$$

where Bo denotes the Boltzmann number:

$$Bo = \frac{\dot{m}_{sp}\bar{c}_{p,sp}}{\sigma\, \psi\, A_k\, T_{ad}^3} \tag{26}$$

An analysis of (25) leads to the conclusion that the flue gas temperature T_{fe} is a function of the Boltzmann number and the furnace chamber emissivity ε_{pal}. A formula with a similar structure is used in standards [11–13]. Based on experimental data obtained from the testing of large power boilers, a new formula containing parameter M, which characterizes the location where the maximum flame temperature occurs in the boiler, was proposed [11]:

$$\frac{T_{fe}}{T_{ad}} = \frac{Bo^{0.6}}{M\, \varepsilon_{pal}^{0.6} + Bo^{0.6}} \tag{27}$$

Parameter M in Eq. (27) is a function of the kind of fuel (oil, gas or coal) and of the relative height at which burners are placed [11–13]. After temperature T_{fe} is calculated from (27), the heat flux $\dot{Q}_r$ absorbed by the furnace chamber walls may be determined. The degree of slagging of the furnace chamber walls may be assessed by determining the waterwall heat efficiency coefficient ψ. It results from an analysis of Eq. (5) that the ψ coefficient gets smaller in proportion to the slagging of the furnace chamber walls. If the furnace chamber walls are covered with a layer of slag, the temperature of the slag surface is high and the density of the heat flux $\dot{q}$ absorbed by the wall (i.e. the wall thermal load) is much smaller than it is with a clean wall. Slagging of the furnace chamber walls results in an increase in the flue gas outlet temperature T_{fe} and a decrease in the heat flux absorbed by the furnace chamber walls $\dot{Q}_r$.

3. Determination of the average degree of furnace chamber fouling

The waterwall heat efficiency coefficient ψ will be determined in an online mode from the following nonlinear equation:

$$\dot{m}_{par}^{zm} = \dot{m}_{par}^{obl}(\psi) \tag{28}$$

where: $\dot{m}_{par}^{zm}$ and $\dot{m}_{par}^{obl}$ denote properly measured and calculated mass flows of steam. The steam mass flow $\dot{m}_{par}^{obl}$ is a function of the waterwall heat efficiency ψ and it is calculated from the boiler evaporator energy balance. The symbol $\dot{m}_{par}^{zm}$ denotes the steam mass flow at the boiler drum outlet determined using the steam mass flow $\dot{m}_p$ measured at the boiler outlet and the water mass flows $\dot{m}_{w1}$ and $\dot{m}_{w2}$ fed into steam attemperators No. 1 and No. 2, respectively.

$$\dot{m}_{par}^{zm} = \dot{m}_p - \dot{m}_{w1} - \dot{m}_{w2} \tag{29}$$

The condition of equality of the calculated and measured values of the steam mass flow allows one to assess the degree of the furnace chamber fouling ζ.

The waterwall heat efficiency coefficient ψ is equal to the product of the waterwall shape factor x, which for tight walls in the OP-380 boiler is equal to unity, multiplied by the fouling coefficient ζ of the chamber furnace heating surfaces:

$$\psi = x\zeta \tag{30}$$

where: $x = 1$ for membrane waterwalls used in the boiler studied.

Determining ζ so that the calculated and measured values of the boiler efficiency are the same, it is possible to assess the average degree of the fouling of the walls of the furnace chamber.

Owing to this way of determining the value of ζ, the temperature of flue gases at the outlet from the furnace chamber T_{fe} may be calculated much more accurately.

If the fouling of the chamber walls is higher, the waterwall efficiency coefficient decreases: $\psi = \zeta$. The heat flux absorbed by the boiler evaporator $\dot{Q}_{par}$ decreases and the flue gas temperature at the furnace chamber outlet increases. As a result, there is a reduction in the steam mass flow generated in the evaporator and directed to the superheaters, which, at a higher flue gas temperature T_{fe}, causes an increment in the reheated steam temperature (at the same mass flow of fuel: $\dot{Q}_{pal}$). In order to maintain the reheated steam temperature at the set level, bigger mass flows of water fed into the reheated steam attemperators are required.

Moreover, the flue gas temperature after individual superheater stages rises due to the fouling of the furnace chamber walls.

The following quantities:

- the waterwall heat efficiency coefficient ψ,
- steam attemperator feed water mass flow rates $\dot{m}_{w1}$ and $\dot{m}_{w2}$,
- the flue gas temperature after individual superheater stages

are strongly dependent on the degree of fouling of the furnace chamber walls. If ψ is reduced, and $\dot{m}_{w1}$ and $\dot{m}_{w2}$, as well as T_{sp}, after individual stages reach permissible set values, the steam slag and ash blowers in the furnace chamber should be activated.

Apart from the above-mentioned indices characterizing the fouling of the boiler heating surfaces in terms of heat exchange, the increase in the flue gas subatmospheric pressure after the superheater stages located further down the convective duct (at a greater distance from the furnace chamber) is another significant symptom of the fouling of the boiler—mainly of the surfaces of superheaters. Increased aerodynamic resistance caused by ash fouling of superheaters leads to higher power consumption by the fan engines. Flue gas pressure and engine power capacity measurements may also be used when assessing the degree of ash fouling of superheaters.

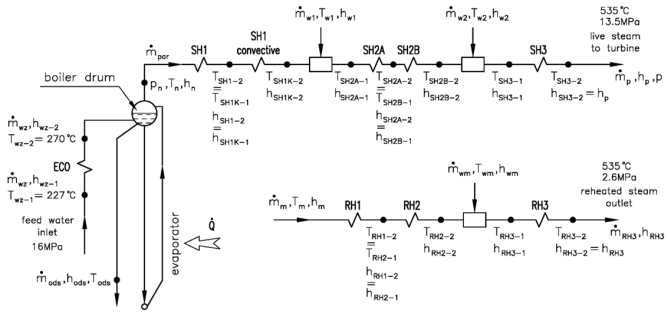

Figure 2: Diagram of control volume for the boiler evaporator mass and energy balance

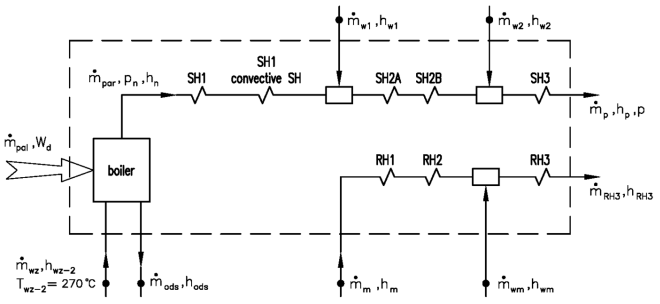

Figure 3: Diagram of control volume for the boiler mass and energy balance

4. Mathematical model of the boiler evaporator

The live steam mass flow is calculated from the boiler evaporator mass and energy balance (Fig. 2):

$$\dot{m}_{wz} = \dot{m}_p - \dot{m}_{w1} - \dot{m}_{w2} + \dot{m}_{ods} \tag{31}$$

$$\begin{aligned} &\dot{m}_{wz} h_{wz-2} + \dot{Q}_{par} = \\ &= \dot{m}_{ods} \cdot h'(p_n) + \left(\dot{m}_p - \dot{m}_{w1} - \dot{m}_{w2}\right) \cdot h''(p_n) \end{aligned} \tag{32}$$

Substitution of (31) in (32) results in:

$$\begin{aligned} \dot{m}_p = {} & \frac{\dot{Q}_{par}}{h"(p_n) - h_{wz-2}} - \dot{m}_{ods} \frac{h'(p_n) - h_{wz-2}}{h"(p_n) - h_{wz-2}} + \\ & + \dot{m}_{w1} + \dot{m}_{w2} \end{aligned} \tag{33}$$

where $\dot{Q}_{par}$ is the heat flux transferred from flue gases to the evaporator via radiation and convection. The heat flux $\dot{Q}_{par}$ may be calculated from the following expression:

$$\dot{Q}_{par} = \dot{Q} - \dot{m}_g \cdot c_{p,g}\Big|_0^{T_{fe}-273.15} \cdot \left(T_{fe} - 273.15\right) \tag{34}$$

where $\dot{Q}$ is the heat flux brought to the furnace chamber with fuel and air, and which is defined as:

$$\dot{Q} = \dot{m}_g \cdot c_{p,g}\Big|_0^{T_{ad}-273.15} \cdot (T_{ad} - 273.15) \tag{35}$$

The symbol T_{fe} denotes the flue gas temperature at the furnace chamber outlet.
The adiabatic combustion temperature is calculated according to Eq. (20).

It should be added that efficiency and thermal calculations require the development of many functions and programs used for the calculation of thermal properties of water, saturated and superheated steam, and flue gases.

5. Determination of fuel mass flow rate

The fuel mass flow rate is calculated based on the fuel chemical composition or on the coal calorific value. The second approach is more appropriate for practical applications, since the chemical composition of the coal is not determined continuously. Boiler efficiency is determined online by the indirect method [6, 14].

Based on the boiler efficiency η determined in an online mode, the coal mass flow is calculated from the definition of the boiler heat efficiency

$$\begin{aligned} \eta = \frac{\dot{Q}_n}{\dot{Q}_h} = {} & \frac{(\dot{m}_p - \dot{m}_{w1} - \dot{m}_{w2})(h_p - h_{wz-2})}{\dot{m}_{pal}\, W_d} + \\ & + \frac{\left[(\dot{m}_{w1} + \dot{m}_{w2}) h_p - \dot{m}_{w1} h_{w1} - \dot{m}_{w2} h_{w2}\right]}{\dot{m}_{pal}\, W_d} + \\ & + \frac{\dot{m}_{ods}(h_n - h_{wz-2})}{\dot{m}_{pal}\, W_d} + \frac{\dot{m}_m (h_{RH1-2} - h_{RH1-1})}{\dot{m}_{pal}\, W_d} + \\ & + \frac{\dot{m}_m (h_{RH2-2} - h_{RH2-1})}{\dot{m}_{pal}\, W_d} + \\ & + \frac{(\dot{m}_m + \dot{m}_{wm})(h_{RH3-2} - h_{RH3-1})}{\dot{m}_{pal}\, W_d} - \\ & - \frac{\dot{m}_{wm} h_{wm}}{\dot{m}_{pal}\, W_d} \end{aligned} \tag{36}$$

The fuel mass flow rate at various boiler loads is determined from Eq. (36) taking into account that the boiler efficiency η is known

$$\begin{aligned} \dot{m}_{pal} = {} & \frac{(\dot{m}_p - \dot{m}_{w1} - \dot{m}_{w2})(h_p - h_{wz-2})}{\eta\, W_d} + \\ & + \frac{\left[(\dot{m}_{w1} + \dot{m}_{w2}) h_p - \dot{m}_{w1} h_{w1} - \dot{m}_{w2} h_{w2}\right]}{\eta\, W_d} + \\ & + \frac{\dot{m}_{ods}(h_n - h_{wz-2})}{\eta\, W_d} + \frac{\dot{m}_m (h_{RH1-2} - h_{RH1-1})}{\eta\, W_d} + \\ & + \frac{\dot{m}_m (h_{RH2-2} - h_{RH2-1}) - \dot{m}_{wm} h_{wm}}{\eta\, W_d} + \\ & + \frac{(\dot{m}_m + \dot{m}_{wm})(h_{RH3-2} - h_{RH3-1})}{\eta\, W_d} \end{aligned} \tag{37}$$

Equations (36) and (37) are valid only for steady state conditions. The symbols: h_{wz-2}, h_n, h_{w1}, h_{w2}, h_{ods}, h_p, h_{RH3} in equations (36) and (37) denote, respectively, the enthalpy of: feed water after the economizer, steam saturated at the boiler drum pressure, injection water in superheated steam attemperators, brine, live steam at the boiler outlet, and reheated steam at the boiler outlet (Fig. 3).

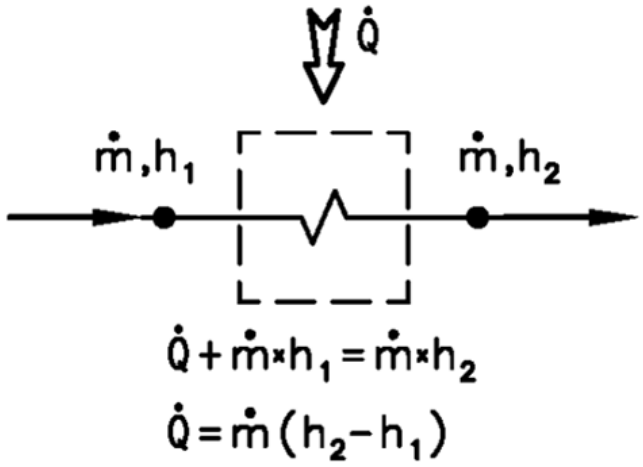

Figure 4: The control area for the superheater energy balance

The calculations of the volume and mass flow rates of the flue gases are based on the determined fuel mass flow rate. Based on the determined excess air number λ using the expression: λ = 21/(21-O_2), defined as the ratio of air to the air flow rate required theoretically, the volume and mass flows of moist flue gases are found. The symbol O_2 denotes the volume fraction of oxygen in the flue gas.

6. Calculation of heat flow rates absorbed by superheater stages and monitoring the degree of fouling of superheaters and reheaters

The degree of fouling of the i-th superheater stage with ash ξ_i is calculated continuously from the following expression:

$$\xi_i = \frac{\dot{Q}_{i,z}}{\dot{Q}_{i,c}} \tag{38}$$

where: $\dot{Q}_{i,z}$, in W, denotes the heat flow rate absorbed by the superheater stage affected by fouling, and $\dot{Q}_{i,c}$, in W, is the heat flow rate absorbed by a clean superheater stage. The heat flow rate $\dot{Q}_{i,c}$ at a given value of the excess air number l is a function of the boiler load. After the boiler is thoroughly cleaned, the measurements of $\dot{Q}_{i,c}$ are made depending on the steam mass flow rate $\dot{m}_i$ flowing through a given superheater stage.

The heat flow rate absorbed by the superheater is determined based on the energy conservation equation. The control area and the method of the superheater energy balance determination is shown in Fig. 4.

The heat flow rates absorbed by individual stages of the live steam superheater in the OP-380 boiler may be determined from the following expressions (Fig. 2):

- platen superheater, which includes wall superheaters which absorb heat flow rate $\dot{Q}_{SH1}$ and hanging platens which absorb heat flow rate $\dot{Q}_{SH1K}$:

$$\dot{Q}_{GR} = \dot{Q}_{SH1} + \dot{Q}_{SH1K} \tag{39}$$

where

$$\dot{Q}_{SH1} = \dot{m}_{par}\,(h_{SH1-2} - h_n) \tag{40}$$

and

$$\dot{Q}_{SH1K} = \dot{m}_{par}\,(h_{SH1K-2} - h_{SH1K-1}) \tag{41}$$

Considering that $h_{SH1-2} = h_{SH1K-1}$ (Figs. 2–3) and substituting equations (40) and (41) into (39), the following expression is obtained:

$$\dot{Q}_{GR} = \dot{m}_{par}\,(h_{SH1K-2} - h_n) \tag{42}$$

- second stage platen superheater

$$\dot{Q}_{SH2} = \left(\dot{m}_{par} + \dot{m}_{w1}\right)(h_{SH2B-2} - h_{SH2A-1}) \tag{43}$$

- third stage (final) superheater

$$\dot{Q}_{SH3} = \left(\dot{m}_{par} + \dot{m}_{w1} + \dot{m}_{w2}\right)(h_{SH3-2} - h_{SH3-1}) \tag{44}$$

Considering that $\dot{m}_{par}+\dot{m}_{w1}+\dot{m}_{w2} = \dot{m}_p$ and $h_{SH3-2} = h_p$, equation (44) assumes the following form:

$$\dot{Q}_{SH3} = \dot{m}_p\left(h_p - h_{SH3-1}\right) \tag{45}$$

The heat flow rates absorbed by individual stages of steam reheaters in the OP-380 boiler may be determined from the following expressions (Figs. 2–3):

- wall reheater

$$\dot{Q}_{RH1} = \dot{m}_m\,(h_{RH1-2} - h_m) \tag{46}$$

- intermediate reheater

$$\dot{Q}_{RH2} = \dot{m}_m\,(h_{RH2-2} - h_{RH2-1}) \tag{47}$$

- final reheater

Table 1: Characteristic of the OP-380 power boiler

Boiler type	With natural circulation
Firing system	Tangential
Output capacity	105.6 kg/s
Live steam temperature	540°C
Live steam pressure	13.9 MPa
Reheated steam temperature	540°C
Reheated steam pressure	2.65 MPa
Feed water temperature	227°C
Boiler efficiency	91%
Fuel type	Hard coal
Fuel low heating value	21.0 MJ/kg

$$\dot{Q}_{RH3} = (\dot{m}_m + \dot{m}_{wm})\,(h_{RH3-2} - h_{RH3-1}) \tag{48}$$

Considering that $\dot{m}_m + \dot{m}_{wm} = \dot{m}_{RH3}$ and $h_{RH3-2} = h_{RH3}$, equation (48) assumes the following form:

$$\dot{Q}_{SH3} = \dot{m}_{RH3}\,(h_{RH3} - h_{SH3-1}) \tag{49}$$

Knowing the heat flow rate $\dot{Q}_{i,c}$ absorbed by the clean i-th stage of the superheat at a given boiler load and heat flow rate $\dot{Q}_{i,z}$ absorbed by the fouled i-th stage at the same load of the boiler, the fouling degree of the i-th superheater stage can be evaluated in the online mode. Pre-setting the limiting value of the fouling degree ξ_i for the i-th superheater stage, the frequency of sootblower activation can be controlled. If the fouling degree ξ_{is} falls below the prescribed limit then the sootblower is activated. Steam and water enthalpies were determined using International Steam Tables [15]. Heat flux measurements using different methods are presented in [16–19].

7. Online monitoring of the steam boiler thermo-flow parameters

The ability to monitor the thermo-hydraulic parameters of steam power boiler is shown through the example of the OP-380 unit used in CHP Krakow S.A. The RAFAKO designed OP-380 steam boiler is a drum type, radiant, pulverized coal fired boiler, with natural circulation. Its characteristics are shown in Table 1.

Figs. 5a and 5b shows the time changes of the fuel and live steam mass flow rates also changes in the excess air ratio and boiler efficiency. Fig. 5a shows the stable operation of the boiler close to nominal capacity.

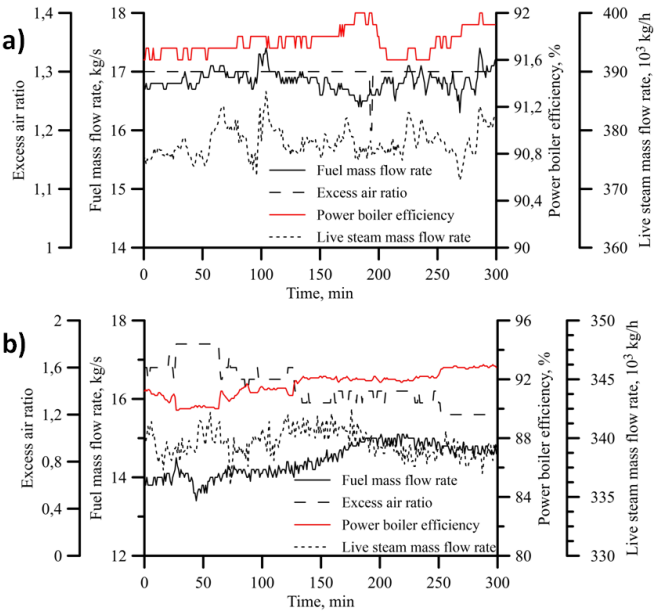

Figure 5: Live steam and fuel mass flow rates, excess air ratio and efficiency of the power boiler time distributions

Throughout the time period the value of the excess air ratio does not change, and boiler efficiency is high—in the range of 91.6–92.0%.

A different situation is presented in Fig. 5b. This figure shows large time variation of the excess air ratio. In the first part of the analyzed interval, the excess air ratio reaches a value of approx. 1.6 which is accompanied by a decrease in boiler efficiency of up to 90%. It is associated with high temperature in the combustion chamber and hence large heat losses in the flue gases. In the second part of the diagram 5b excess air ratio decreases to 1.2, which is a typical value for this type of boiler. This situation is reflected in an increase in boiler efficiency to above 92%.

Heat flow rates received by the power boiler evaporator (Fig. 6), live steam superheater (Fig. 7) and steam reheater are also monitored.

Online monitoring of the heat flux received by the steam boiler heating surfaces can be used to assess the degree of fouling and slagging of the combustion chamber and live steam superheater. Any increase in the fouling of the combustion chamber is reflected by a decrease in live steam flow. This information can be a signal for the operator to start the boiler water or steam sootblowers.

8. Conclusion

A method for determining the thermal and flow parameters of a steam power boiler was presented in the paper.

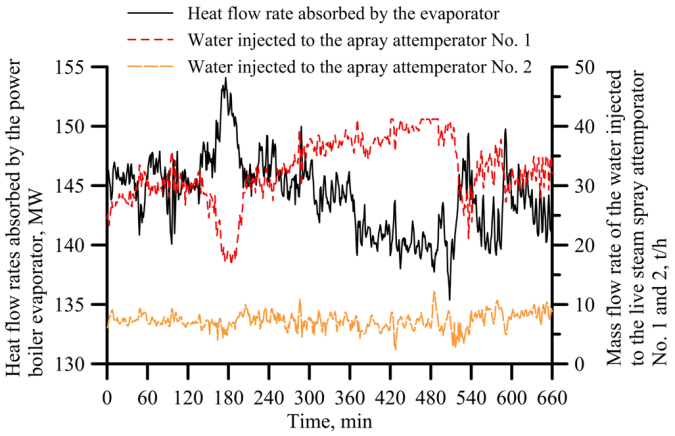

Figure 6: Time distribution of the heat flow rate absorbed by the boiler's evaporator

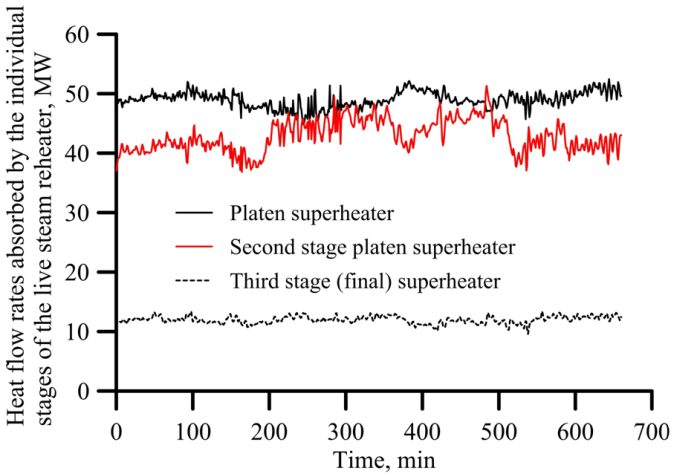

Figure 7: Time distribution of the heat flow rates absorbed by the live steam superheater stages

This method allows one to perform online calculations of the boiler furnace chamber and heat flow rates absorbed by superheater stages. These parameters are important for the monitoring of the power unit operation and make it possible to determine the degree of the furnace chamber slagging and to operate the steam boiler at high efficiency. The ability to monitor thermal and flow parameters has been shown on an example OP−380 power boiler.

References

[1] H. Bilirgen, Slagging in pc boilers and developing mitigation strategies, Fuel 115 (2014) 618–624.

[2] N. Harding, D. O'Connor, Ash deposition impacts in the power industry, Fuel Processing Technology 88 (11) (2007) 1082–1093.

[3] L. M. Romeo, R. Gareta, Hybrid system for fouling control in biomass boilers, Engineering Applications of Artificial Intelligence 19 (8) (2006) 915–925.

[4] L. M. Romeo, R. Gareta, Fouling control in biomass boilers, Biomass and bioenergy 33 (5) (2009) 854–861.

[5] A. Syed, N. Simms, J. Oakey, Fireside corrosion of superheaters: Effects of air and oxy-firing of coal and biomass, Fuel 101 (2012) 62–73.

[6] J. Taler, M. Trojan, D. Taler, Monitoring of Ash Fouling and Internal Scale Deposits in Pulverized Coal Fired Boilers, Nova Science Publishers, New York, 2011.

[7] J. C. Stępień, A. Salij, M. E. Poniewski, Impact of biomass co-firing on selected parameters of a 225 mw power unit, Journal of Power Technologies 95 (Polish Energy Mix 2014) (2015) 84–90.

[8] H. Othman, J. Purbolaksono, B. Ahmad, Failure investigation on deformed superheater tubes, Engineering Failure Analysis 16 (1) (2009) 329–339.

[9] A. K. Ray, Y. Tiwari, R. Sinha, P. Roy, S. Sinha, R. Singh, S. Chaudhuri, Remnant life assessment of service-exposed pendent superheater tubes, Engineering Failure Analysis 9 (1) (2002) 83–92.

[10] P. Madejski, D. Taler, Analysis of temperature and stress distribution of superheater tubes after attemperation or sootblower activation, Energy Conversion and Management 71 (2013) 131–137.

[11] N. Kuznetsov, W. Mitor, I. Dubovski, E. Karasina, Thermal calculations of steam boilers. standard method, Energia: Moscow, Russia.

[12] A. Blokh, Heat transfer in steam boiler furnaces, hemisphere, Washington, DC.

[13] S. Kakac, Boilers, evaporators, and condensers, John Wiley & Sons, 1991.

[14] J. Taler (Ed.), Thermal and flow processes in large steam boilers. Modeling and monitoring, WNT Scientific and Technical Publishing, Warsaw, 2011, in Polish.

[15] W. Wagner, H. J. Kretzschmar, International Steam Tables Properties of Water and Steam Based on the Industrial Formulation IAPWS-IF97, Springer-Verlag, Berlin, 2008.

[16] J. Taler, D. Taler, P. Ludowski, Measurements of local heat flux to membrane water walls of combustion chambers, Fuel 115 (2014) 70–83.

[17] J. Taler, D. Taler, Heat Flux: Processes, Measurement Techniques and Applications, Nova Science Publishers, New York, 2012, Ch. Measurement of heat flux and heat transfer coefficient, pp. 1–104.

[18] P. Duda, J. Taler, A new method for identification of thermal boundary conditions in water-wall tubes of boiler furnaces, International Journal of Heat and Mass Transfer 52 (5–6) (2009) 1517–1524.

[19] J. Taler, D. Taler, Heat Transfer, InTech, Rijeka–Shanghai, 2012, Ch. Measurements of Local Heat Flux and Water-Side Heat Transfer Coefficient in Water Wall Tubes, pp. 3–34.